

Expanded View Figures

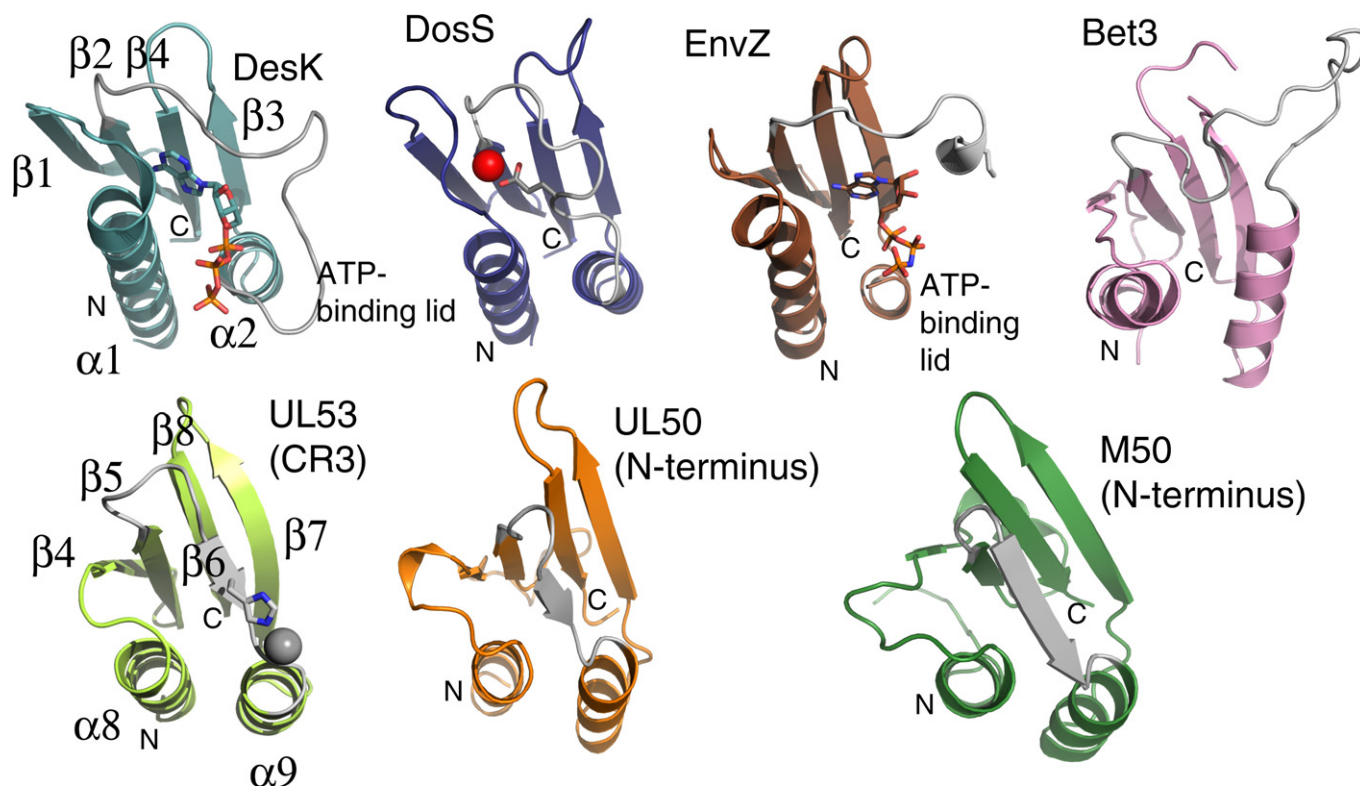


Figure EV1. Structural comparison of the conserved Bergerat fold in UL50 and UL53 with that of members of the GHKL superfamily and Bet3.

Ribbon representations of (from left to right in the top row) the ATP-binding domains of three histidine kinase proteins (DesK, DosS, and EnvZ). The ATP molecules bound in DesK and EnvZ are shown in stick form, and the ATP-binding lid is shown in gray. A short linker region (gray) on which a glutamate residue (in part) coordinates zinc (red sphere) takes the place of an ATP-binding lid in DosS. The ATP-binding lid is also missing in a portion of Bet3, a vesicle-trafficking protein (top row, right), and the NEC subunits (bottom row, left to right) UL53 (comprising most of conserved region 3 (CR3)), and UL50 and M50, both comprising the N-terminal portion of the proteins, where otherwise the Bergerat fold (α - β - β - α - β - β topology) is fully conserved (the secondary elements of DesK and UL53 are labeled as an example of the fold sequence). The deviations observed between the structures at the ATP-binding lid or equivalent region are shown in gray.

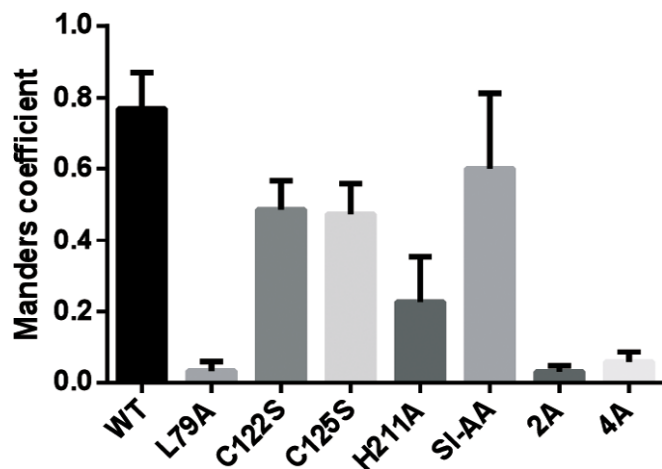


Figure EV2. Quantitation of UL50 and UL53 co-localization in cells.

Co-localization analysis between wild-type and mutant versions of HA-tagged UL50 or FLAG-UL53 in cells using Fiji/ImageJ. The Manders M1 coefficients were calculated for multiple cells of each sample within a defined region of interest (ROI) proximal to the nucleus and summarized in a bar graph. The values represent the mean and the error bars depict the standard deviation (\pm SD).

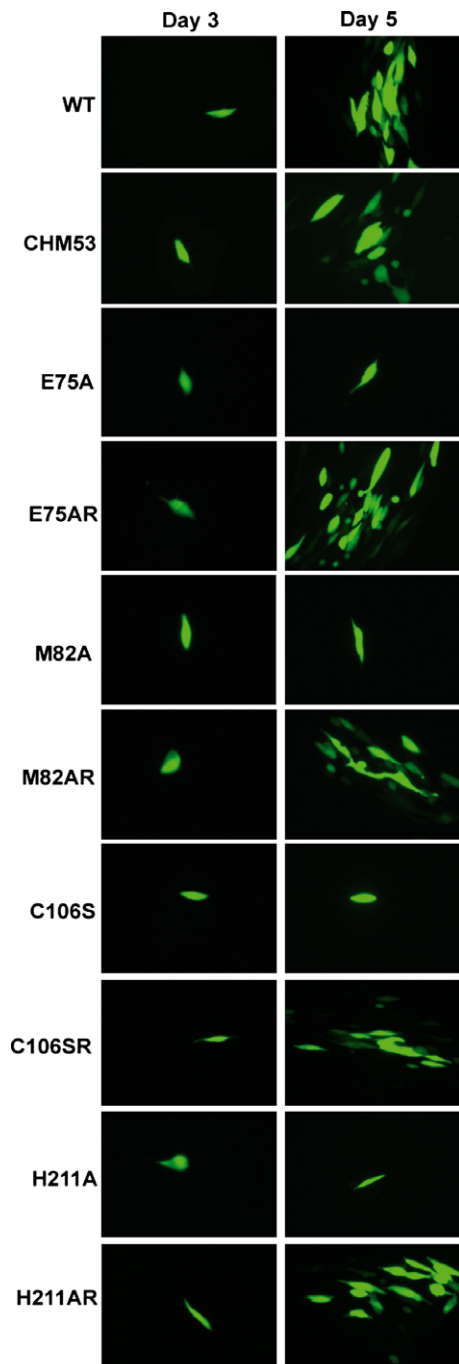


Figure EV3. Effects of mutations on the zinc finger and the amphiphatic helices of UL53 on HCMV viability.

Human foreskin fibroblasts (HFFs) electroporated with HCMV BACs that express GFP, and either WT UL53, UL53 mutants, or their rescued derivatives as indicated to the left of each panel, were imaged at day 3 or 5 post-electroporation to monitor the spread of the virus infection in the cell monolayer.

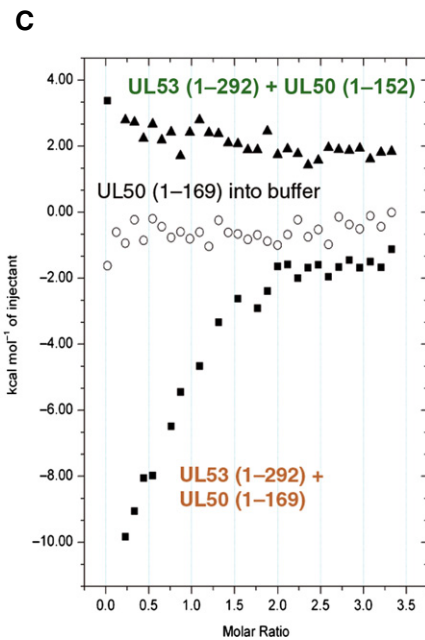
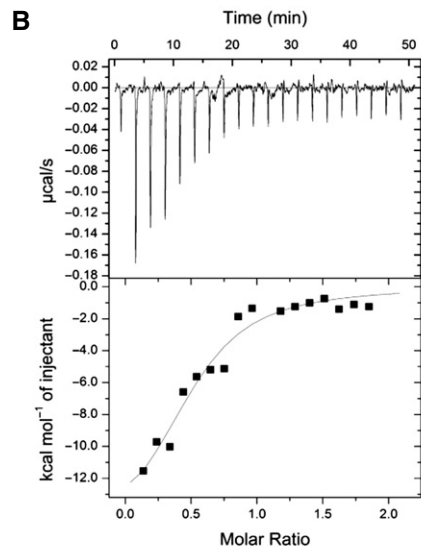
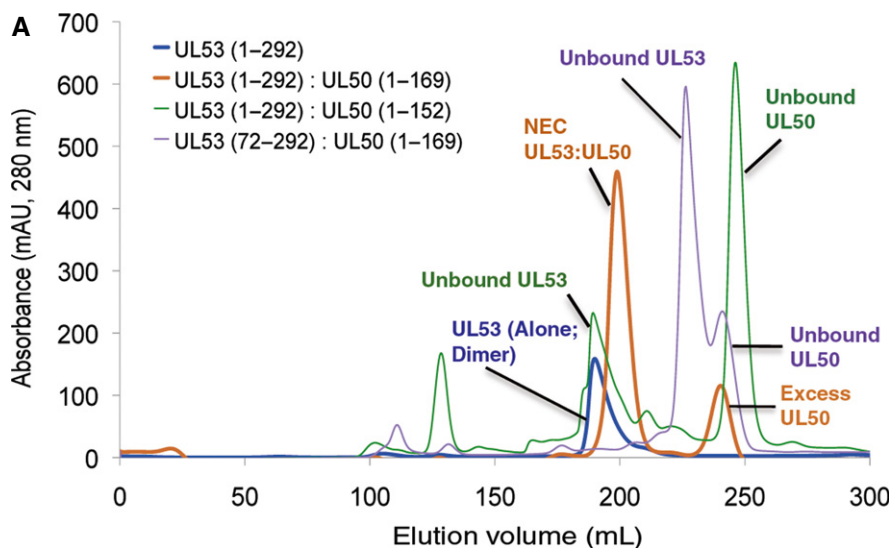


Figure EV4. The N-terminal amphiphatic helices on UL53 and the C-terminal helix of UL50 are required for NEC formation.

A Column chromatography testing the ability of UL50 and UL53 truncation mutants to form the NEC. UL53-encompassing residues 1–292 (UL53^{1–292}) alone elute as a homodimer (blue). Incubation of a 1:3 ratio of UL53^{1–292} with UL50^{1–169} results in complete binding of UL53 to form a heterodimer with excess UL50 eluting as a monomer (orange). A C-terminal truncation mutant of UL50 (UL50^{1–152}), however, is unable to bind to UL53^{1–292}, and each protein elutes separately, with UL53^{1–292} as a homodimer and UL50 as a monomer (green). A similar result is observed with UL53^{72–292}, an N-terminal truncation mutant, with both proteins eluting separately as unbound monomeric proteins (purple). Unlike UL53^{1–292}, UL53^{72–292} is a monomer, similar to UL53^{84–292} (Sam *et al.*, 2009).

B ITC studies of binding of Chm53 to UL50^{1–169}. The K_d derived was $1.0 \pm 0.08 \mu\text{M}$.

C ITC studies of binding of UL53^{1–292} with UL50^{1–169} (labeled in orange) or UL50^{1–152} (labeled in green), the binding isotherms of which are shown as squares and triangles, respectively. The isotherm for UL50^{1–169} titrated into buffer is shown in circles. The K_d derived for UL53^{1–292} with UL50^{1–169} was $3.8 \pm 0.8 \mu\text{M}$.

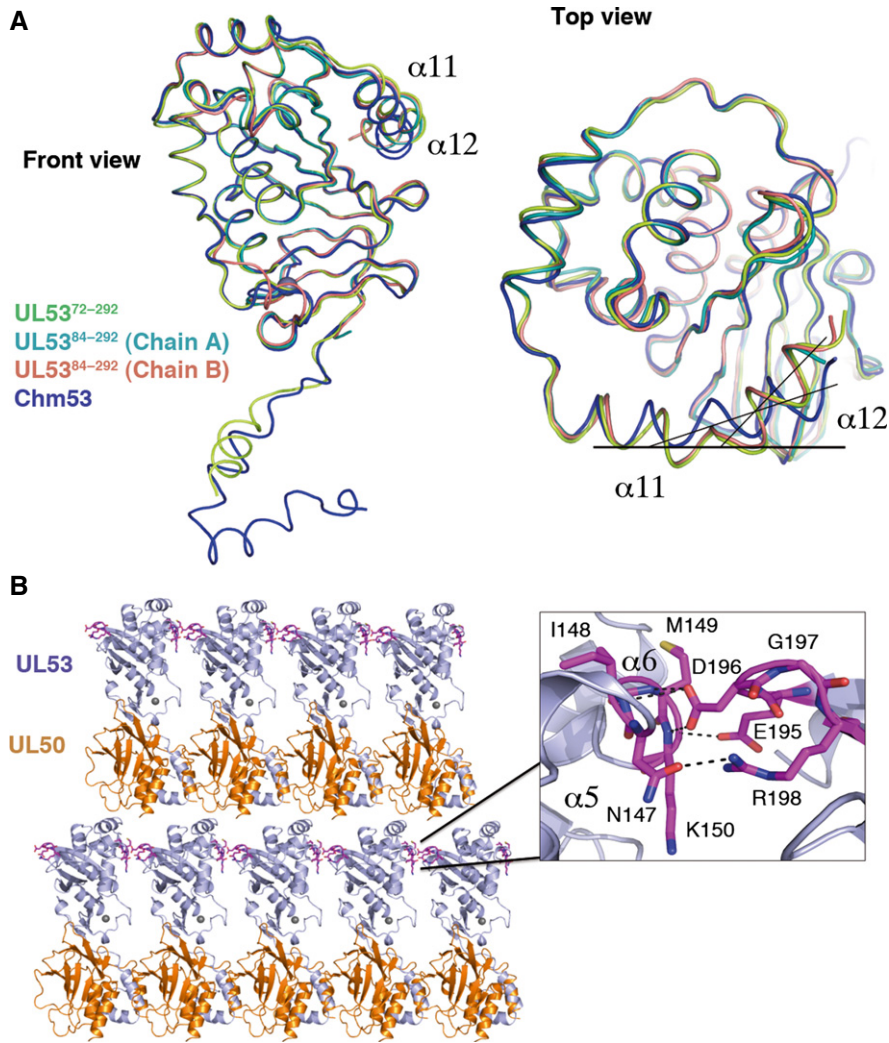


Figure EV5. Crystal packing of UL53 and the NEC.

A Comparison of the C-terminal helices in the UL53 structures. The C-terminus tail ($\alpha 11$ and $\alpha 12$) of the UL53-only structures comprising residues 72–292 (UL53⁷²⁻¹⁶⁹, limon), which crystallized in the P4 space group, and UL53⁸⁴⁻²⁹² [both chains A (cyan) and B (salmon)], which crystallized in the P1 space group, overlay almost perfectly (front view and top view). These structures have a bend of $\sim 145^\circ$ between $\alpha 11$ and $\alpha 12$. In contrast, however, the bend flattens to $\sim 170^\circ$ between $\alpha 11$ and $\alpha 12$ of Chm53 (blue) from the NEC structure, which crystallized in the C2 space group (top view).

B Lateral contacts mediating NEC crystal packing. A close-up view of the extensive hydrogen bonding interactions (dashed black lines) between the residues on $\alpha 5$ and $\alpha 6$ on one molecule (left), with residues between $\beta 4$ and $\beta 5$ of a neighboring molecule (right). The interacting residues are shown in magenta.